Electronic Supplementary Material (ESI) for Soft Matter.

Supplementary Information

Ouzo phase occurrence with alternated lipo/hydrophilic copolymers in water

Henrique Trevisan[1], Kana Nishimori[2], Stefano Aime[1], Jean-Michel Guigner[3], Makoto Ouchi[2] and Francois Tournilhac[1].*

[1]Molecular, Macromolecular Chemistry, and Materials, CNRS, UMR 7167, ESPCI-Paris, PSL Research University, 10 rue Vauquelin 75005, France

[2] Department of Polymer Chemistry, Graduate School of Engineering, Kyoto University, Katsura Nishikyo-ku, Kyoto 615-8510, Japan

[3] Institut de Minéralogie, de Physique des Matériaux et de Cosmochimie, Sorbonne Université, CNRS, UMR 7590, IRD, MNHN, 4 place Jussieu, F-75005 Paris, France

* Correspondence to: francois.tournilhac@espci.fr

Contents

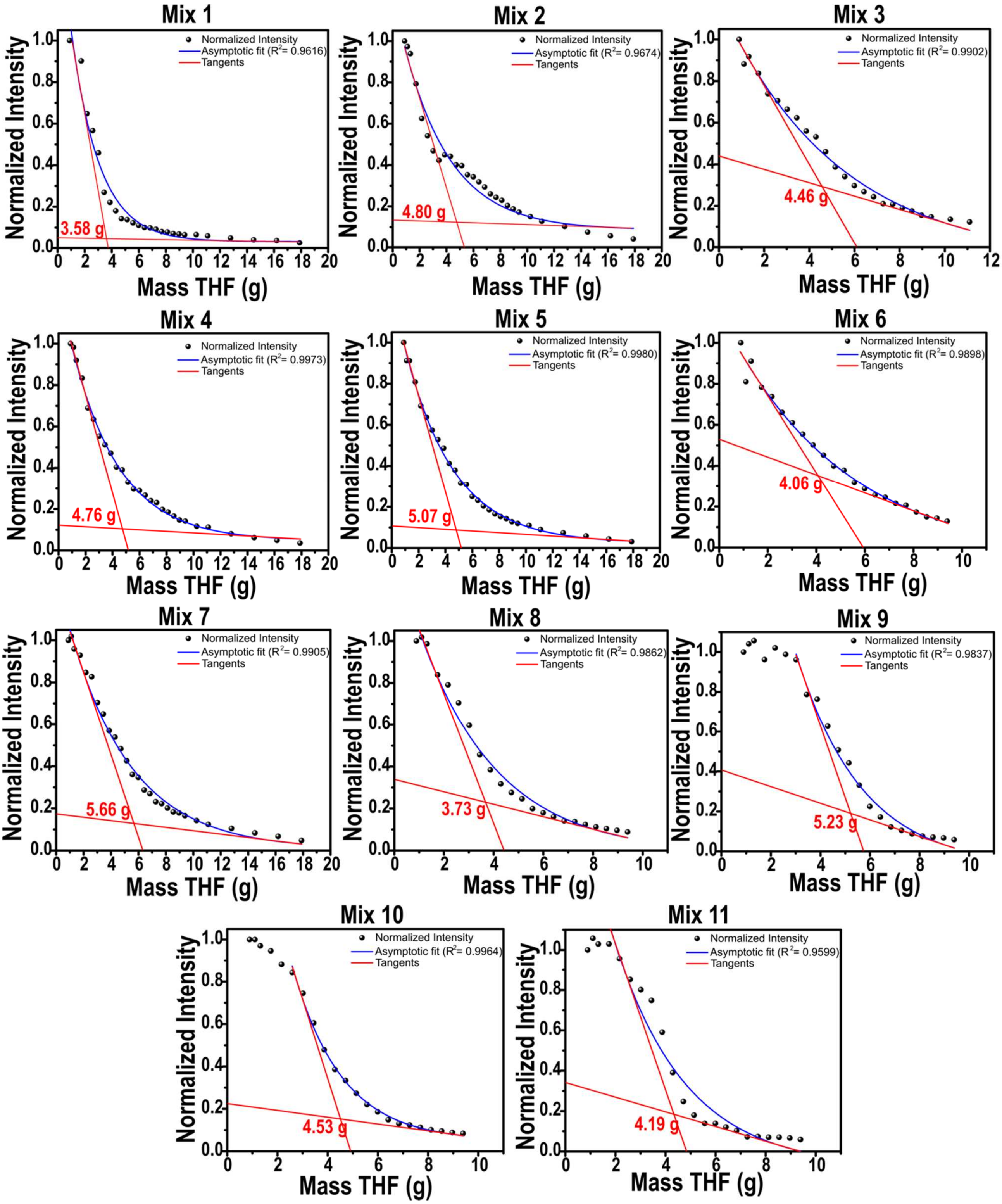

Fig. S1 Determination of miscibility limit (Binodal points) using sequential addition of solvent (THF) to a dispersion of nanoparticles of **AltC12** previously prepared with increasing initial copolymer mass fractions from (Mix 1 to Mix 11). Initial mass fractions and binodal points are shown in Table S1. The intensity of scattered light (at 90°) decreases asymptotically close to the binodal limit, which is determined by using the crossing points of the tangents at the beginning and at the end of the asymptotic curves.

Table S1. Initial **AltC12** mass fractions for preparation of nanoparticles in the ouzo region and respective binodal points determined via titration with THF.

		Binodal Points		
Mixture	**Initial AltC12 mass fraction (x 10^{-3})**	**F_{water}**	**F_{THF}**	**F_{AltC12} (x 10^{-4})**
1	0.250	0.583	0.417	1.514
2	0.254	0.510	0.489	1.527
3	0.354	0.530	0.470	2.214
4	0.406	0.513	0.487	2.455
5	0.491	0.497	0.503	2.876
6	0.584	0.556	0.443	3.821
7	0.661	0.469	0.531	3.656
8	0.767	0.571	0.428	5.168
9	0.832	0.488	0.511	4.888
10	0.908	0.532	0.467	5.673
11	1.008	0.546	0.453	6.487

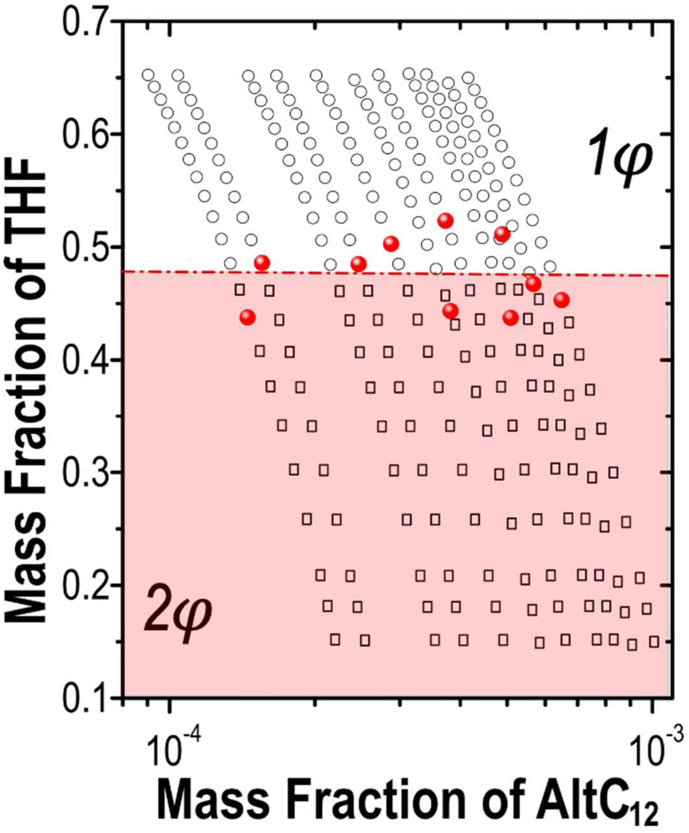

Fig. S2 Miscibility limit determined via THF addition to **AltC12** nanoparticle suspensions. Squares are the compositions of the mixtures in the ouzo region and circles are mixtures in the one phase region (solutions).

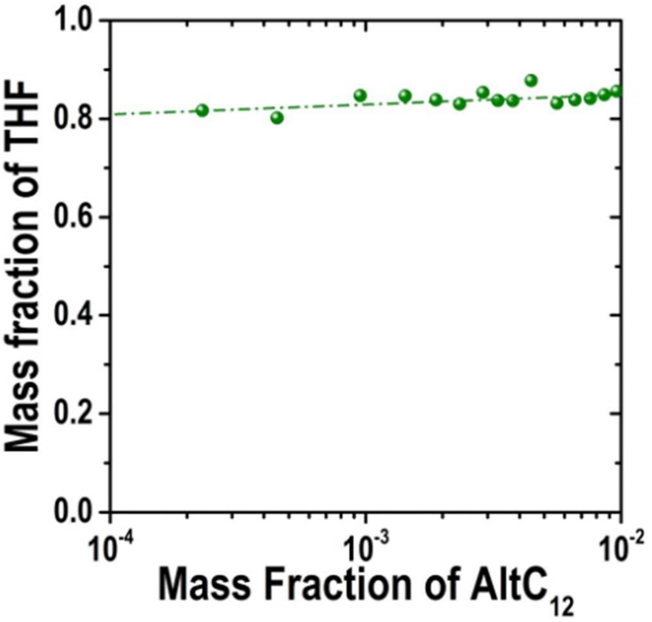

Fig. S3 Miscibility limit determined via H_2O addition to **AltC12** solutions in THF. The binodal line determination using this 'direct' technique relies on visual detection of turbidity upon sequential addition of non-solvent to the copolymer solution. Comparison of Fig. S2 and Fig S3 reveals that the whole transition line may be shifted towards higher or lower solvent fraction, depending on detection technique utilized.

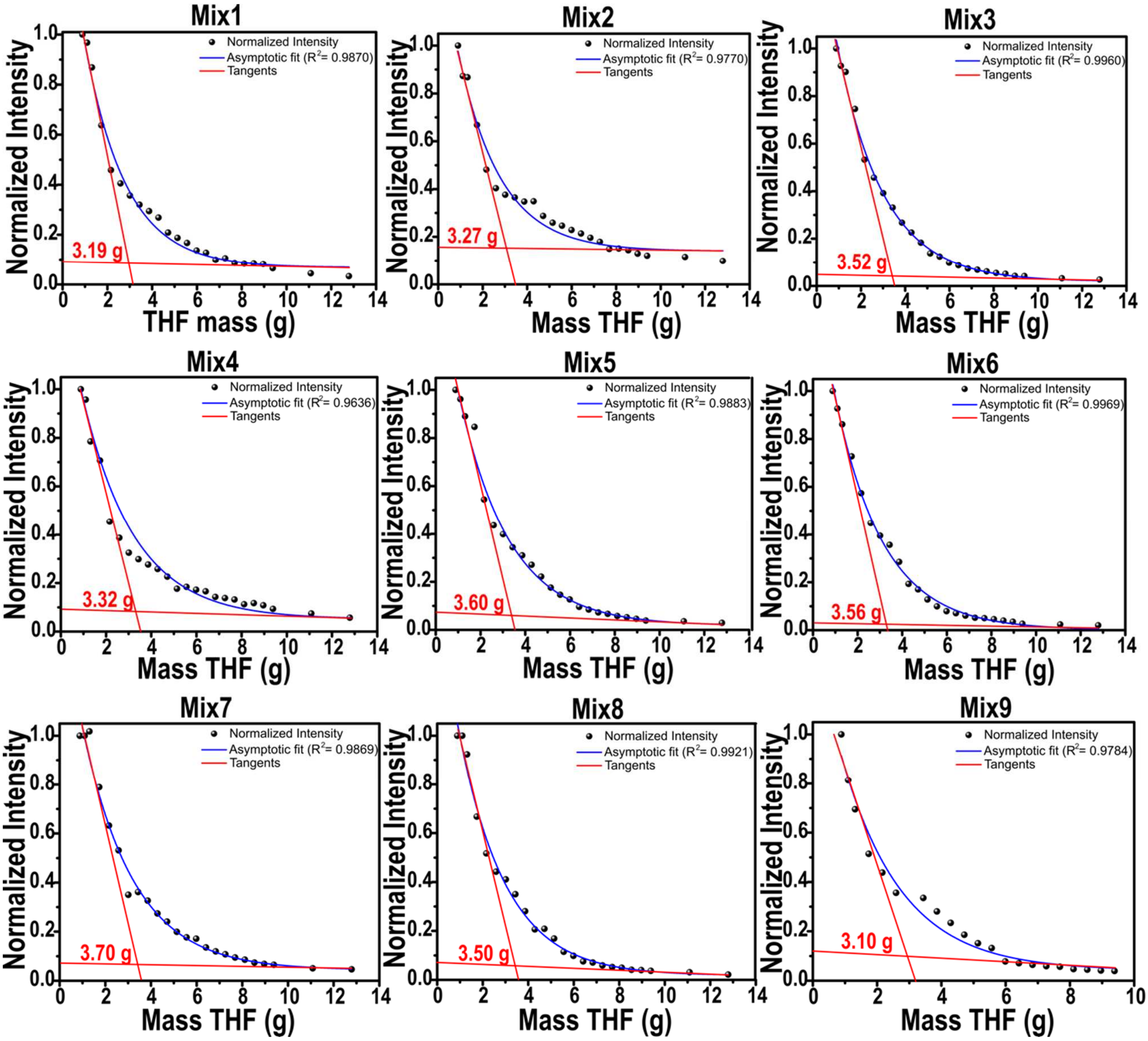

Fig. S4 Determination of miscibility limit (Binodal points) using sequential addition of solvent (THF) to a dispersion of nanoparticles of **AltC18** previously prepared with increasing initial copolymer mass fractions from (Mix 1 to Mix 9). Initial mass fractions and binodal points are shown in Table S2. The intensity of scattered light (at 90°) decreases asymptotically close to the binodal limit, which is determined by using the crossing points of the tangents at the beginning and at the end of the asymptotic curves.

Table S2. Initial **AltC18** mass fractions for preparation of nanoparticles in the ouzo region and respective binodal points determined via titration with THF.

		Binodal Points		
Mixture	**Initial AltC18 mass fraction (x 10^{-3})**	**F_{water}**	**F_{THF}**	**F_{AltC18} (x 10^{-4})**
1	0.135	0.613	0.387	0.971
2	0.169	0.614	0.386	1.180
3	0.220	0.587	0.412	1.523
4	0.254	0.602	0.398	1.797
5	0.322	0.582	0.418	2.206
6	0.440	0.585	0.415	3.029
7	0.521	0.578	0.422	3.534
8	0.592	0.589	0.411	4.109
9	0.676	0.618	0.382	4.925

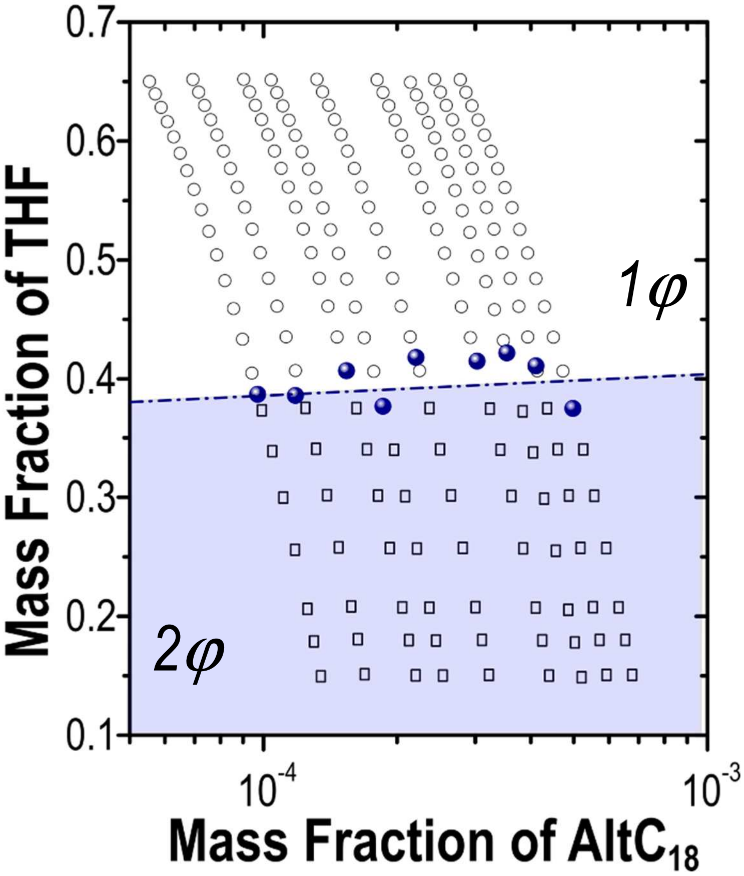

Fig. S5 Miscibility limit determined via THF addition to **AltC18** nanoparticle suspensions. Squares are the compositions of the mixtures in the ouzo region and circles are mixtures in the one phase region (solutions).

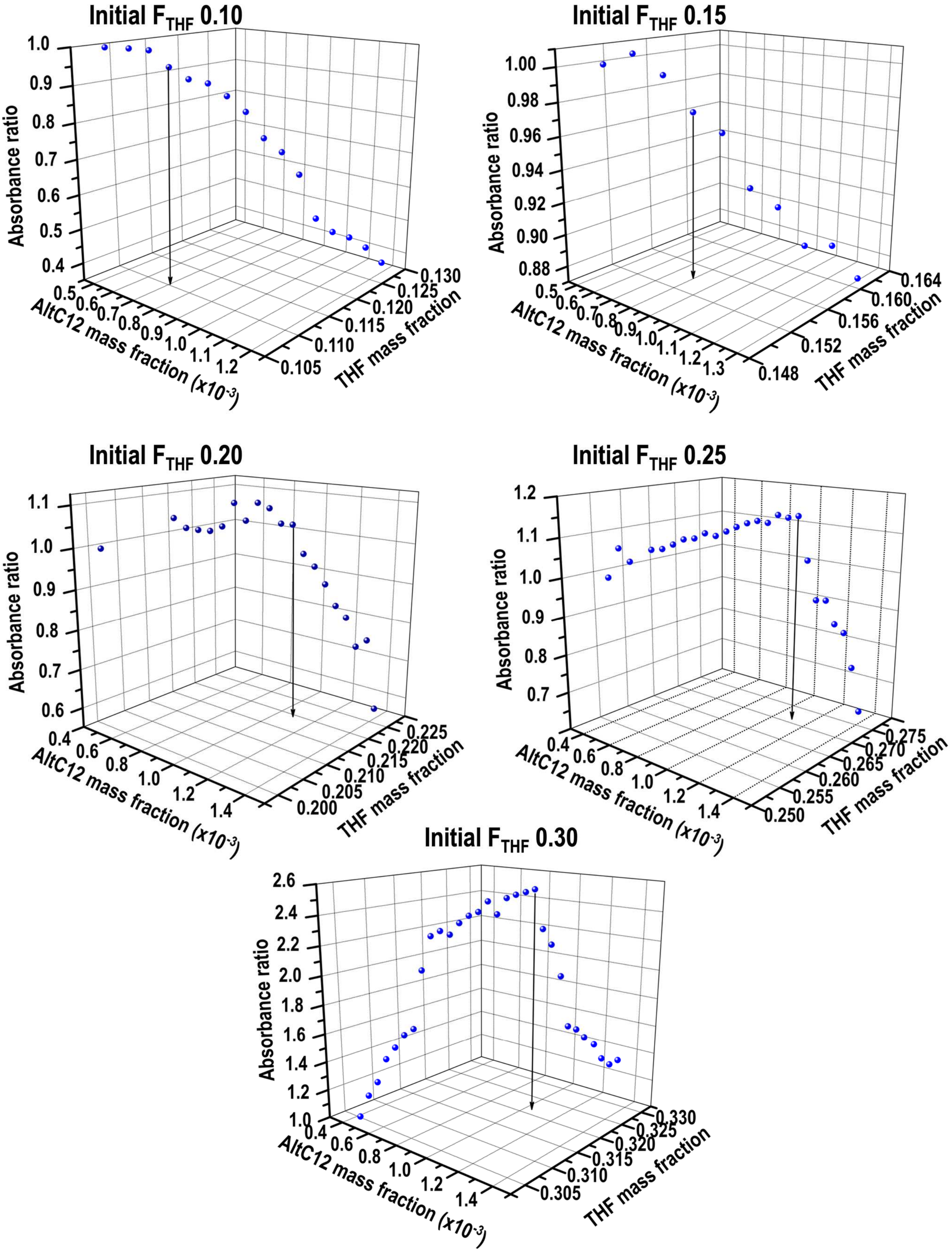

Initial F_{THF} 0.10

Initial F_{THF} 0.15

Initial F_{THF} 0.20

Initial F_{THF} 0.25

Initial F_{THF} 0.30

Fig. S6 Determination of the Ouzo stability points for **AltC12** using the measurement of optical density at λ= 600 nm before and after sequential addition of copolymer solution in the system. Once macroscopic aggregates are formed, they separate from the bulk of the suspension resulting on the decrease of the absorbance ratio ($Abs_{final}/Abs_{initial}$). For samples with high initial THF mass fractions the absorbance ratio increases in the beginning due to the increase of the size of the initial nanoparticles.

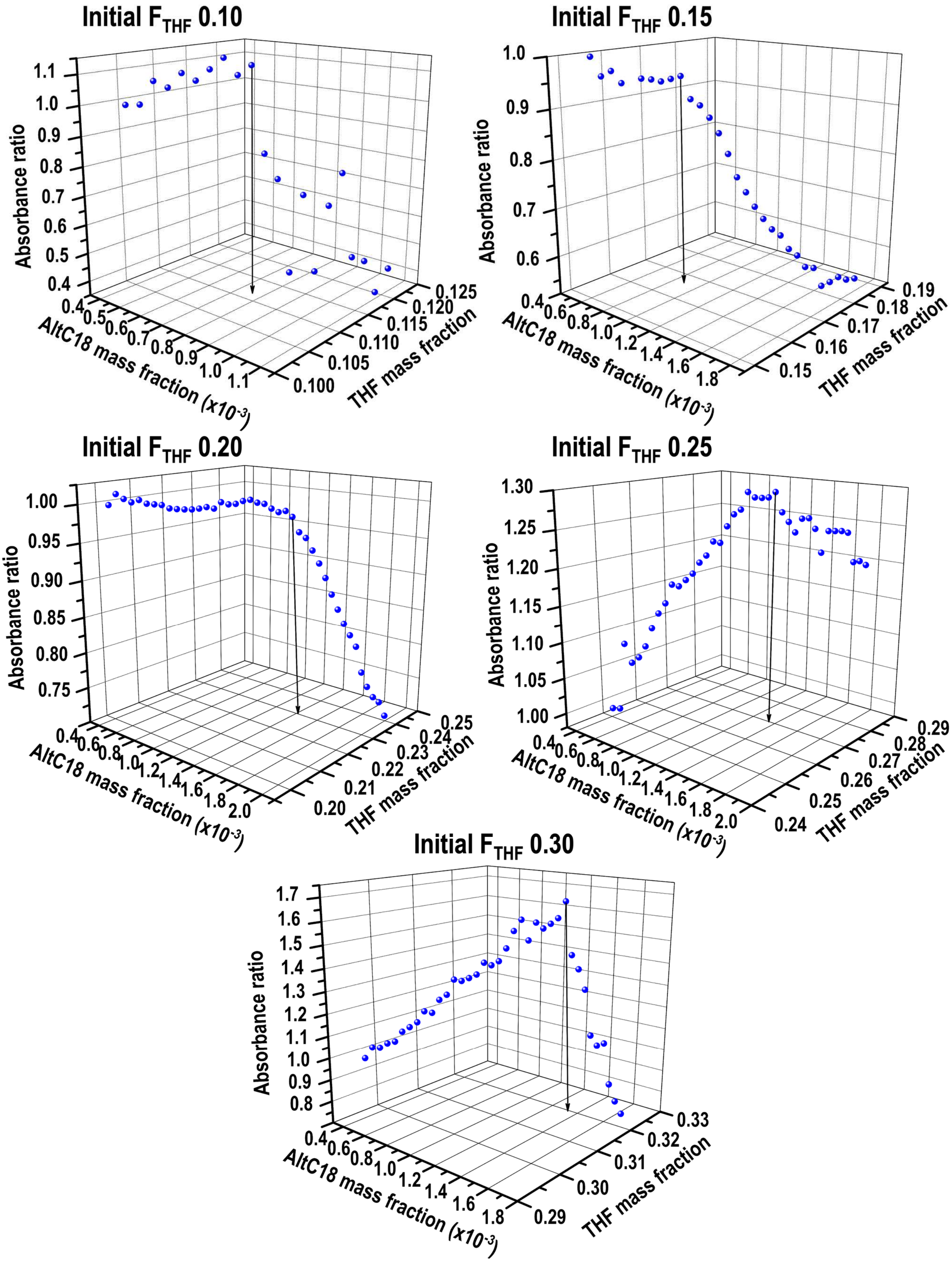

Fig. S7 Determination of the Ouzo stability points for **AltC18** using the measurement of optical density at λ= 600 nm before and after sequential addition of copolymer solution in the system. Once macroscopic aggregates are formed, they separate from the bulk of the suspension resulting on the decrease of the absorbance ratio (Abs$_{final}$/Abs$_{initial}$). For samples with high initial THF mass fractions the absorbance ratio increases in the beginning due to the increase of the size of the initial nanoparticles.

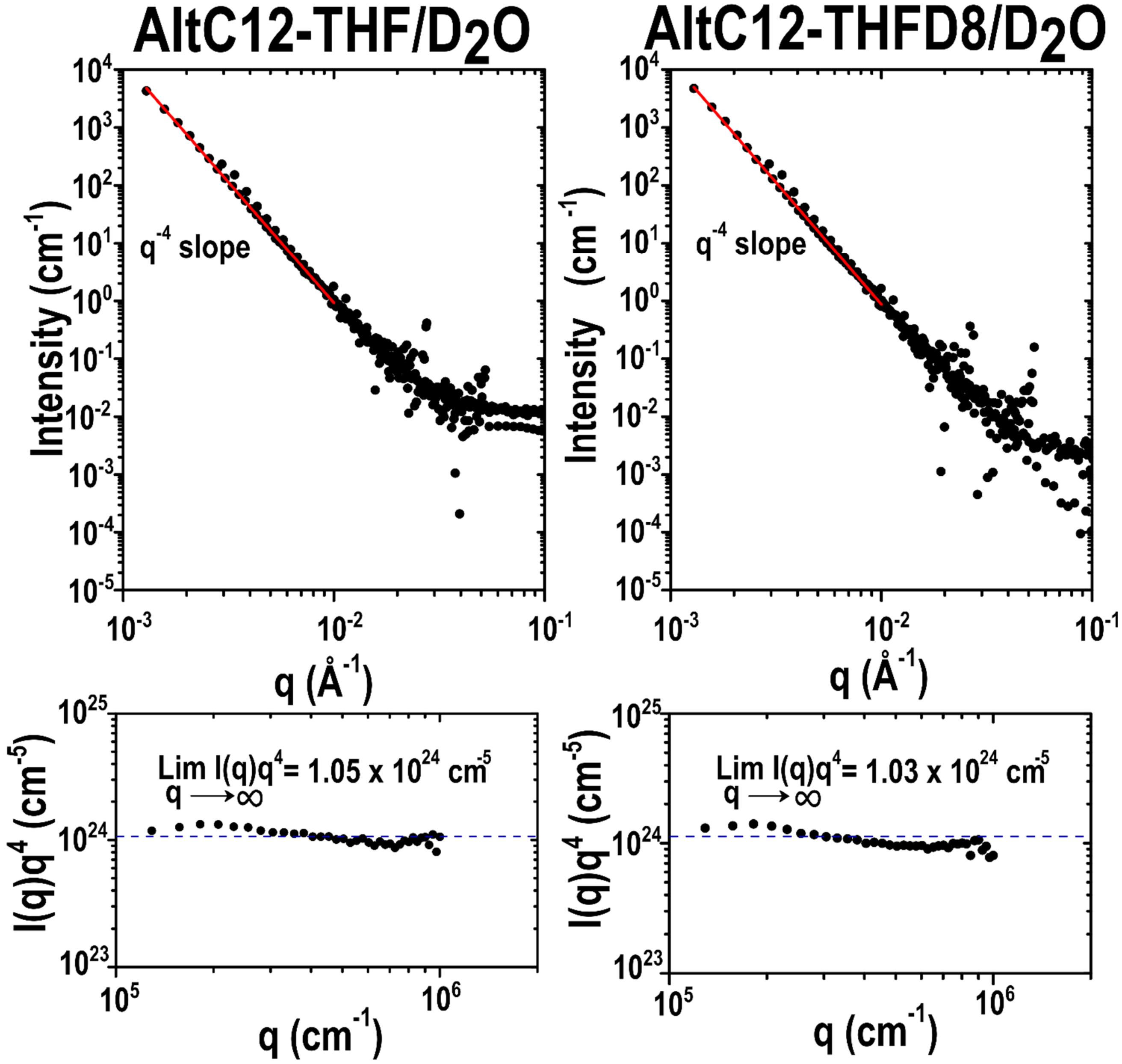

Fig. S8 Log – Log plot of SANS data in absolute intensity I(q) vs q for the copolymer nanoparticles in non-deuterated solvent (**AltC12-THF/D$_2$O**) and deuterated solvent (**AltC12-THFD8/D$_2$O**), respectively. The raw intensity data as corrected for background and the Porod's limit was calculated for q^{-4} slope regime to determine the specific area interface and the radius of the copolymer nanoparticles.

THF-d8/D_2O

Model name: core shell sphere
χ^2 : 90.02
Scale: 4.5 10^{-4} **(fixed)**
Background: 0.04
Outermost radius: 3700 Å
Thickness: 1250 Å
SLD_core: 5.34×10^{-6} Å^{-2}
SLD_shell: 0.54×10^{-6} Å^{-2} **(fixed)**
SLD_solvent mix: 6.33×10^{-6} Å^{-2}

THF/D_2O

Model name: core shell sphere
χ^2 : 217
Scale: 4.5 10^{-4} **(fixed)**
Background: 0.11
Outermost radius: 3700 Å **(constrained)**
Thickness: 1250 Å **(constrained)**
SLD_core: 0.93×10^{-6} Å^{-2}
SLD_shell: 0.54×10^{-6} Å^{-2} **(fixed)**
SLD_solvent mix: 5.77×10^{-6} Å^{-2}

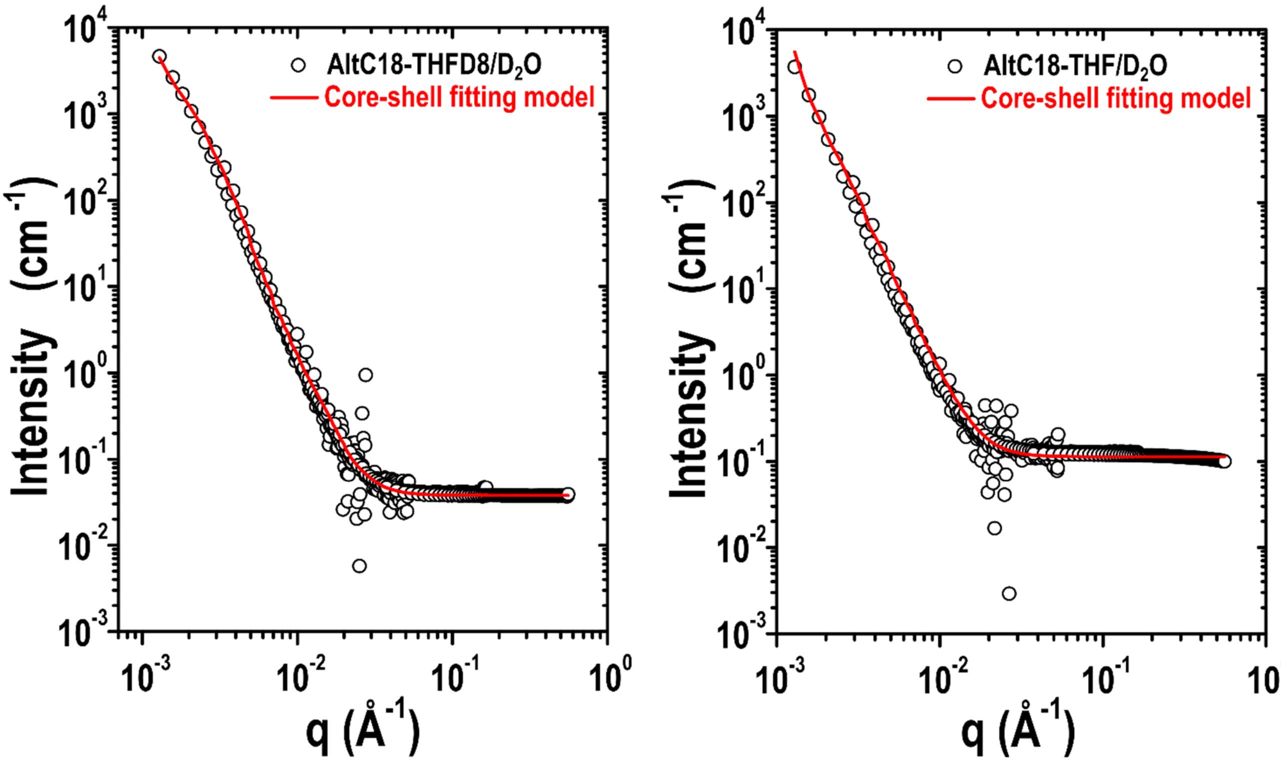

Fig. S9 Log – Log plot of SANS data in absolute intensity I(q) vs q for the copolymer nanoparticles in deuterated solvent (**AltC18-THFD8/D_2O**) and non-deuterated solvent (**AltC18-THF/D_2O**), respectively. The scattering intensity data were fitted with core shell model using the constrained fit on SasView software with pinhole smearing resolution of dq/q = 0.25. Scale and SLD_shell are the two fixed values for the determination of the radius, thickness, SLD_core and SLD_solvent.

The intensity detected in a scattering experiment can be expressed as the square modulus of a scattering amplitude $\mathrm{A(q)}$, which is generally related to the Fourier transform of the local scattering length density[1]: $\mathrm{A(q)} = \mathrm{A_0} \int_{\mathrm{V}} \rho(\vec{\mathrm{x}}) e^{-\mathrm{i}\vec{\mathrm{q}}\cdot\vec{\mathrm{x}}} \mathrm{d}^3\vec{\mathrm{x}}$, where $\mathrm{A_0}$ is a prefactor dependent on details of the scattering instrument such as the source intensity, the cross-sectional area of the detector and its distance from the sample; $\rho(\vec{\mathrm{x}})$ is the scattering length density, in units of 1/length^2, and the integral runs over the whole scattering volume V. When the scattering

---

[1] A. Guinier, and G. Fournet, Small-angle scattering of X-rays, Wiley, New York (1955)

medium is composed of a set of N discrete particles, the integral can be divided into a sum of single-particle terms:

$$A(q) = A_0 \sum_{j=1}^{N} \left[\int_{V_j} \Delta\rho(\vec{x}_j) e^{-i\vec{q}\cdot\vec{x}_j} d^3\vec{x}_j \right] e^{-i\vec{q}\cdot\vec{X}_j} = A_0 \sum_{j=1}^{N} b_j(\vec{q}) e^{-i\vec{q}\cdot\vec{X}_j}$$

Where now $\Delta\rho(\vec{x}_j)$ denotes the contrast in scattering length density of the particle relative to the background medium (the solvent). Each term of the sum represents the contribution of j-th particle, of volume V_j and center of mass $\vec{X}_j$, such that $\vec{x}_j = \vec{x} - \vec{X}_j$. The integral defines the scattering length of j-th particle $b_j(\vec{q}) = \int_{V_j} \Delta\rho(\vec{x}_j) e^{-i\vec{q}\cdot\vec{x}_j} d^3\vec{x}_j$.

If $\Delta\rho(\vec{x})$ is homogeneous inside the particle, it can be factored out of the integral. For a spherical particle, the integral yields:[2] $b_j^{(sph)}(\vec{q}) = \Delta\rho V_j 3 j_1(qr_j)/(qr_j)$, where r_j is the radius of the sphere, $V_j = 4\pi r_j^3/3$ and $j_1(x) = (\sin x - x\cos x)/x^2$ is the first spherical Bessel function of the first kind. The scattering length of a core-shell spherical particle with outer (shell) radius r_s and inner (core) radius r_c can be computed by expressing the integral as a sum of two homogeneous spheres: one with radius r_s and density contrast $\Delta\rho_s = \rho_{shell} - \rho_{solvent}$ and another with radius r_c and density contrast $\Delta\rho_c = \rho_{core} - \rho_{shell}$. The result yields: $b_j^{(cs)}(\vec{q}) = \Delta\rho_s V_s 3 j_1(qr_s)/(qr_s) + \Delta\rho_c V_c 3 j_1(qr_c)/(qr_c)$, where $V_{c,s} = 4\pi r_{c,s}^3/3$.

Absolute (static) scattered intensities can be obtained by normalizing the ensemble-averaged $|A(q)|^2$ by the instrument-dependent prefactor A_0 and the scattering volume V.[3] The result has units of an inverse length:

$$I(q) = \frac{1}{V} \langle \sum_{j=1}^{N} \sum_{k=1}^{N} b_j(\vec{q}) b_k^*(\vec{q}) e^{-i\vec{q}\cdot(\vec{X}_j - \vec{X}_k)} \rangle$$

where $\langle \cdots \rangle$ denotes the ensemble average, equivalent to a time average if the sample is ergodic. The double sum can be split into a “self” term (with $j = k$), in which the argument is simply $|b_j(q)|^2$, and a “cross” term ($j \neq k$), which vanishes if the particles have no positional correlation, as the phase factors are randomly distributed around zero [2]. Thus, for identical core-shell particles one gets:

$$I(q) = \frac{N}{V} |b(q)|^2$$

$$= \frac{N}{V} \left[3V_s(\rho_{shell} - \rho_{solvent}) \frac{\sin(qr_s) - qr_s\cos(qr_s)}{(qr_s)^3} + 3V_c(\rho_{core} - \rho_{shell}) \frac{\sin(qr_c) - qr_c\cos(qr_c)}{(qr_c)^3} \right]^2$$

---

[2] A. Guinier, Theorie et technique de la radiocristallographie, 3e Ed, Dunod, Paris (1964)

[3] P. Pusey, Introduction to Scattering Experiments, in: P. Lindner, and Th. Zemb, Neutrons, X-rays and Light: Scattering Methods Applied to Soft Condensed Matter, North-Holland (2002)

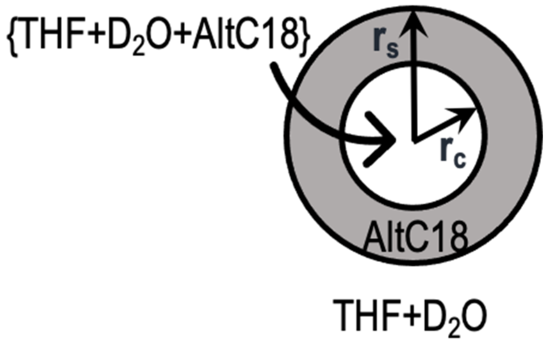

According to the SANS data and the constrained fitting, the values of ρ_{core} (SLD_core) indicate, in both cases, that inside the nanoparticles there is a mixture of copolymer, water and THF. Considering that the SLD of the mixture can be calculated from the fractions (χ) of each component and their respective scattering length densities, we have:

i) $\rho_{core} = \chi_{D2O}\rho_{D2O} + \chi_{THF}\rho_{THF} + \chi_{AltC18}\rho_{AltC18}$
ii) $1 = \chi_{D2O} + \chi_{THF} + \chi_{AltC18}$

From the fitting of **AltC18-THFD8/D$_2$O** and **AltC18-THF/D$_2$O,** we have two values for ρ_{core}:

(**AltC18-THFD8/D$_2$O**) = 5.34 x10^{10}(cm^{-2})
(**AltC18-THF/D$_2$O**) = 0.93 x10^{10}(cm^{-2})

Therefore, we a have a linear system with three independent variables and three equations:

i) $5.34 = \chi_{D2O}6.33 + \chi_{THFd8}6.35 + \chi_{AltC18}0.54$
ii) $0.93 = \chi_{D2O}6.33 + \chi_{THF}0.18 + \chi_{AltC18}0.54$
iii) $1 = \chi_{D2O} + \chi_{THF} + \chi_{AltC18}$

Solutions:

$$\chi_{D2O} = \frac{13313}{119081};\ \chi_{THF} = \frac{441}{617};\ \chi_{AltC18} = \frac{20655}{119081}$$

Approximate values:

$$\chi_{D2O} = 0.1118;\ \chi_{THF} = 0.7147;\ \chi_{AltC18} = 0.1735$$

Therefore, it is possible to infer that during the solvent-shift process of AltC18 in THF to H$_2$O, core-shell like structures are formed with an average radius of 370 nm, in which the core is a mixture of 11.18% of water; 71.47% of THF and 17.35% of copolymer and the shell of 125 nm thickness is consisted of AltC18.